

**Corrosion of Mild Steel in High CO<sub>2</sub> Environment: Effect of the FeCO<sub>3</sub> Layer**

M. F. Suhor, M.F. Mohamed, A. Muhammad Nor, M. Singer and S. Nesic  
Institute for Corrosion and Multiphase Flow,  
Ohio University, Athens, OH 45701

**ABSTRACT**

In the oil and gas industry, transportation of the hydrocarbons may involve high concentrations of CO<sub>2</sub> and significant amounts of liquid water which will provide the electrolyte for the corrosion of mild steel to take place. The consequent damage can be in the form of general corrosion or localized – pitting attack. However at these conditions, an iron carbonate (FeCO<sub>3</sub>) layer may form which can provide some level of protection. The current work undertakes a study of the corrosion behavior of mild steel in high partial pressure CO<sub>2</sub> system, which covers all three states of CO<sub>2</sub>: gas, liquid and supercritical. The transient behaviors of the CO<sub>2</sub> corrosion process is revealed, with corrosion rates changing from extreme initial values to very low corrosion rates due to a FeCO<sub>3</sub> layer forming.

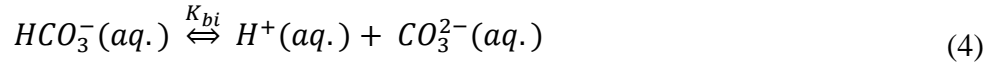
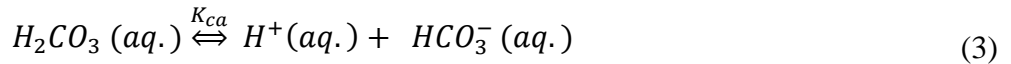
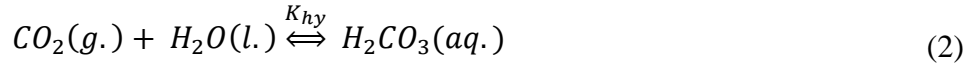
Key words: High pCO<sub>2</sub>, Iron carbonate, FeCO<sub>3</sub>, and passive layer.

**INTRODUCTION**

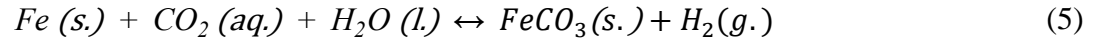
Mild steel is the most obvious material for many engineering applications on the basis of its low cost, availability, good weldability, excellent mechanical properties, etc. However it is not very resistant to corrosion attack which can cause structural integrity issues. The most common corrosive species encountered in oil and gas industry is carbonic acid; a byproduct of reaction between CO<sub>2</sub> gas and water. South East Asia including Malaysia was recognized to have large gas fields that contain high concentration of CO<sub>2</sub> up to 90%<sup>[1]</sup>.

Mass loss in the form of general corrosion is generally proportional to CO<sub>2</sub> partial pressure and temperature<sup>[2]</sup>. However it was also well documented that at certain conditions i.e. pH above 6 and elevated temperature will promote a precipitation layer on the steel surface, identified as iron carbonate (FeCO<sub>3</sub>)<sup>[3]</sup>. This layer has a mitigating effect on CO<sub>2</sub> corrosion<sup>[4]</sup>.

Processes involving CO<sub>2</sub> can be described by a set of chemical and electrochemical reactions. At ambient condition, CO<sub>2</sub> will exist as a gas. This is the most common phase encountered in the field. CO<sub>2</sub> will readily dissolve in water, followed by its hydration to form carbonic acid and dissociation to form hydrogen ions, bicarbonate and carbonate ions. These processes are shown by reactions (1) – (4) below:<sup>[5]</sup>



The overall reaction of iron from the steel in an aqueous CO<sub>2</sub> environment corresponds to:



The precipitation of FeCO<sub>3</sub> (s) layer is only possible once the combined concentration of Fe<sup>2+</sup> and CO<sub>3</sub><sup>2-</sup> exceed the solubility limit to give supersaturation (SS), according to:

$$SS = \frac{C_{Fe^{2+}} * C_{CO_3^{2-}}}{K_{sp}}$$

The solubility limit proposed by Sun, *et al.*,<sup>[6]</sup> which took into consideration the temperature effects as well as the ionic strength of the bulk solution is:

$$\log K_{sp} = -59.3498 - 0.041377 \times T - \frac{2.1963}{T} + 24.5724 \times \log(T) + 2.518 \times I^{0.5} - 0.657 \times I$$

where:

$K_{sp}$  - solubility constant

$T$  - temperature

$I$  - ionic strength

It is known that the precipitation rate is a function of temperature as well as species concentration. The following equation can be used to describe the precipitation rate of FeCO<sub>3</sub>. [7], [8].

$$R_{FeCO_3(s)} = \frac{A}{V} \times f(T) \times K_{sp} \times f(SS)$$

where:

$A/V$  - area to volume ratio

$f(T)$  and  $f(SS)$  - functions defined in <sup>[7]</sup>, <sup>[8]</sup>

## EXPERIMENTAL PROCEDURE

The experiment was conducted in a newly built 20 liters autoclave (see Figure 1). This autoclave is capable to hold in high test pressure up to 100 bars. However, initially a series of preliminary tests was conducted in the autoclave at atmospheric pressure for comparison against glass cell results and validation of the new experimental setup. Only then was the autoclave pressurized for the main set of experiments described below.

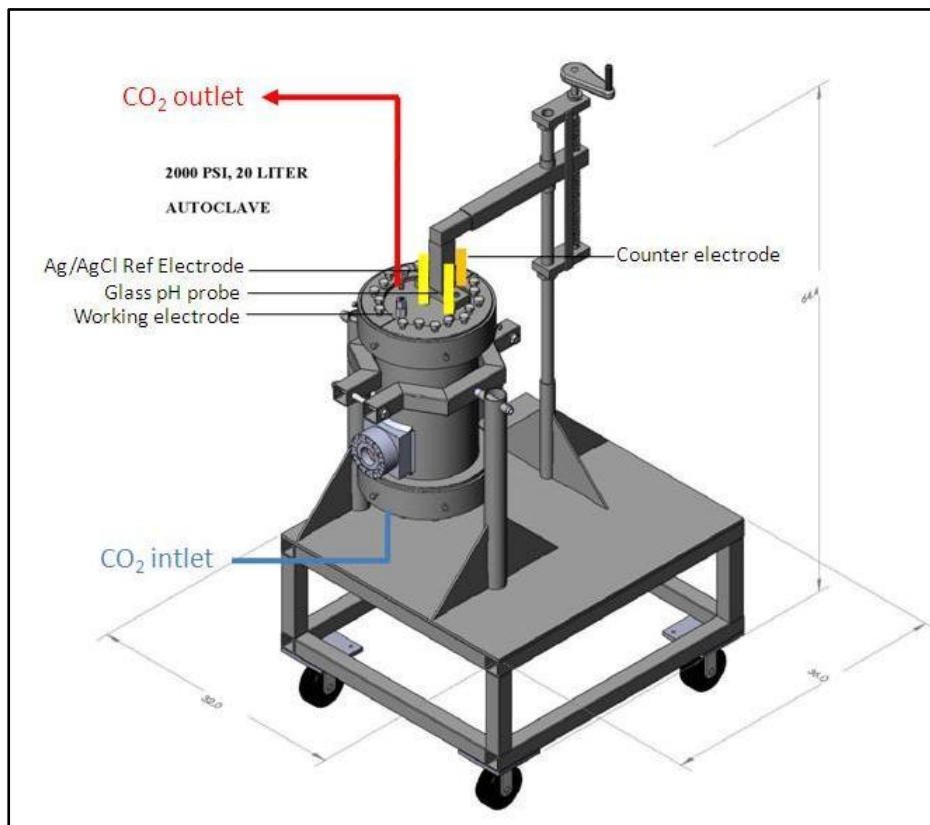


**Figure 1:** Autoclave for corrosion testing in high pressure and high temperature condition

Three electrodes setup connected to a potentiostat was used for the electrochemical measurement. These specially designed electrode are capable of withstand high pressure (up to 2000 psi) and high temperature (150°C). The working electrode (WE) consists of cylindrical specimen made of carbon steel (API 5L X65). The reference electrode (RE) was a high pressure and high temperature probe with a built in Ag/AgCl element. The same reference electrode was also used to help measure pH. The counter electrode (CE) was very similar to WE, however it was coated with platinum.

The following test matrix was designed to look into the effect of  $\text{FeCO}_3$  layer buildup on mild steel corrosion in high  $p\text{CO}_2$  environment.

**Table 1:** Test matrix for the corrosion experiments - mild steel in high  $p\text{CO}_2$  environments.

| Parameters                | Value  |
|---------------------------|--|
| Electrolyte               | 1 wt.% NaCl                                  |
| Temperature               | 25, 50 & 80°C                                |
| Pressure of $\text{CO}_2$ | 10, 20, 40, 60 & 80 bar                      |
| pH                        | Autogenous                                   |
| Flow                      | Stagnant                                     |
| Method                    | Electrochemical and weight loss measurements |
| Duration                  | 1 to 30 days                                 |

A high pressure high temperature (HPHT) pH probe was used to monitor the changes of water chemistry during the experiments. Dissolved iron concentration was measurement using UV light spectroscopy.

## RESULTS

The test matrix covered a wide range of parameters and conditions involving gas, liquid and supercritical CO<sub>2</sub>. Results shown in this paper represent those phases accordingly:

- Condition 1; 10 bar and 25°C - the CO<sub>2</sub> in a gas phase
- Condition 2; 80 bar and 25°C - the CO<sub>2</sub> in a liquid phase
- Condition 3; 10 bar and 80°C - the CO<sub>2</sub> in a gas phase at high temperature
- Condition 4; 80 bar and 80°C - the CO<sub>2</sub> in a supercritical phase

The results indicate that in Condition 1 and 2 no change in corrosion behavior with time occurred over the duration of the experiments, as shown in the Figure 2. However, in Condition 3 and 4 changes of the corrosion rate with time is clear.

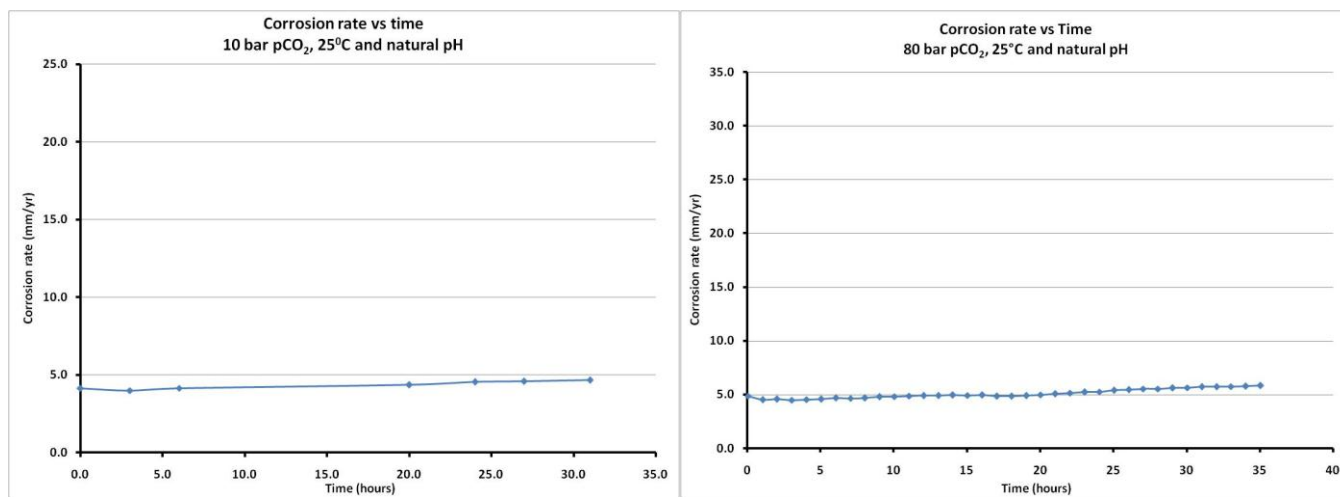


**Figure 2:** Corrosion rate of X65 mild steel measured using the Linear Polarization Resistance (LPR) method at Conditions 1 and 3.  $T=25^{\circ}\text{C}$  and  $p\text{CO}_2 = 10$  and 80 bar.

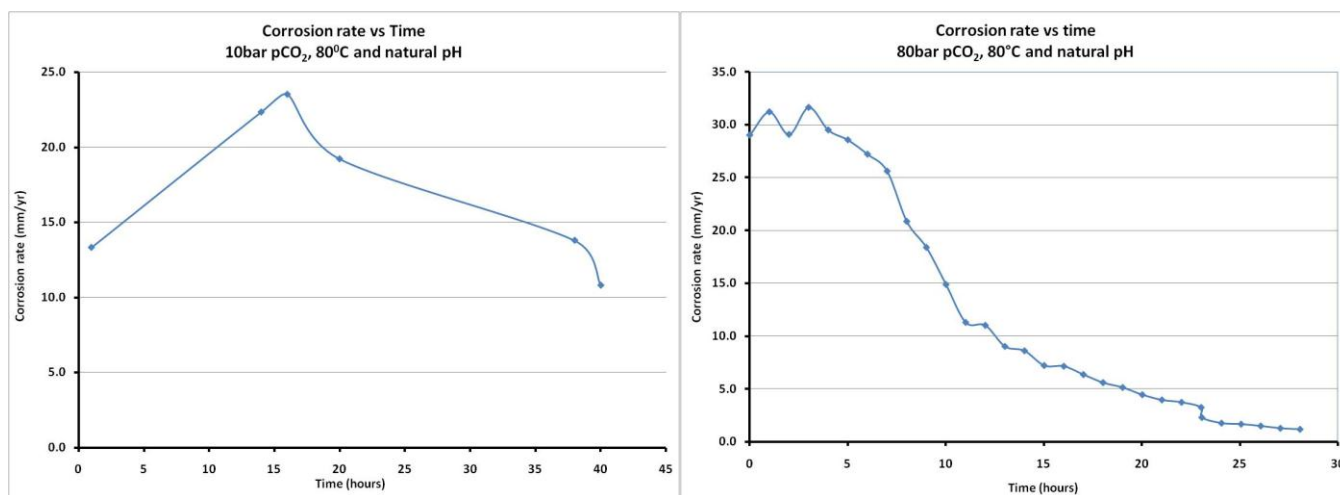


**Figure 3:** Corrosion rate of X65 mild steel measured using Linear Polarization Resistance (LPR) method at Conditions 3 and 4.  $T=80^{\circ}\text{C}$  and  $p\text{CO}_2 = 10$  and 80 bar.

Post experimental analysis of the steel specimen surface using Scanning Electron Microscopy (SEM) has revealed the presents of  $\text{FeCO}_3$  in high temperature test only i.e. at  $80^\circ\text{C}$ . It was observed that the coverage by the  $\text{FeCO}_3$  crystal was more thorough at  $p\text{CO}_2 = 80$  bar than at  $p\text{CO}_2 = 10$  bar.

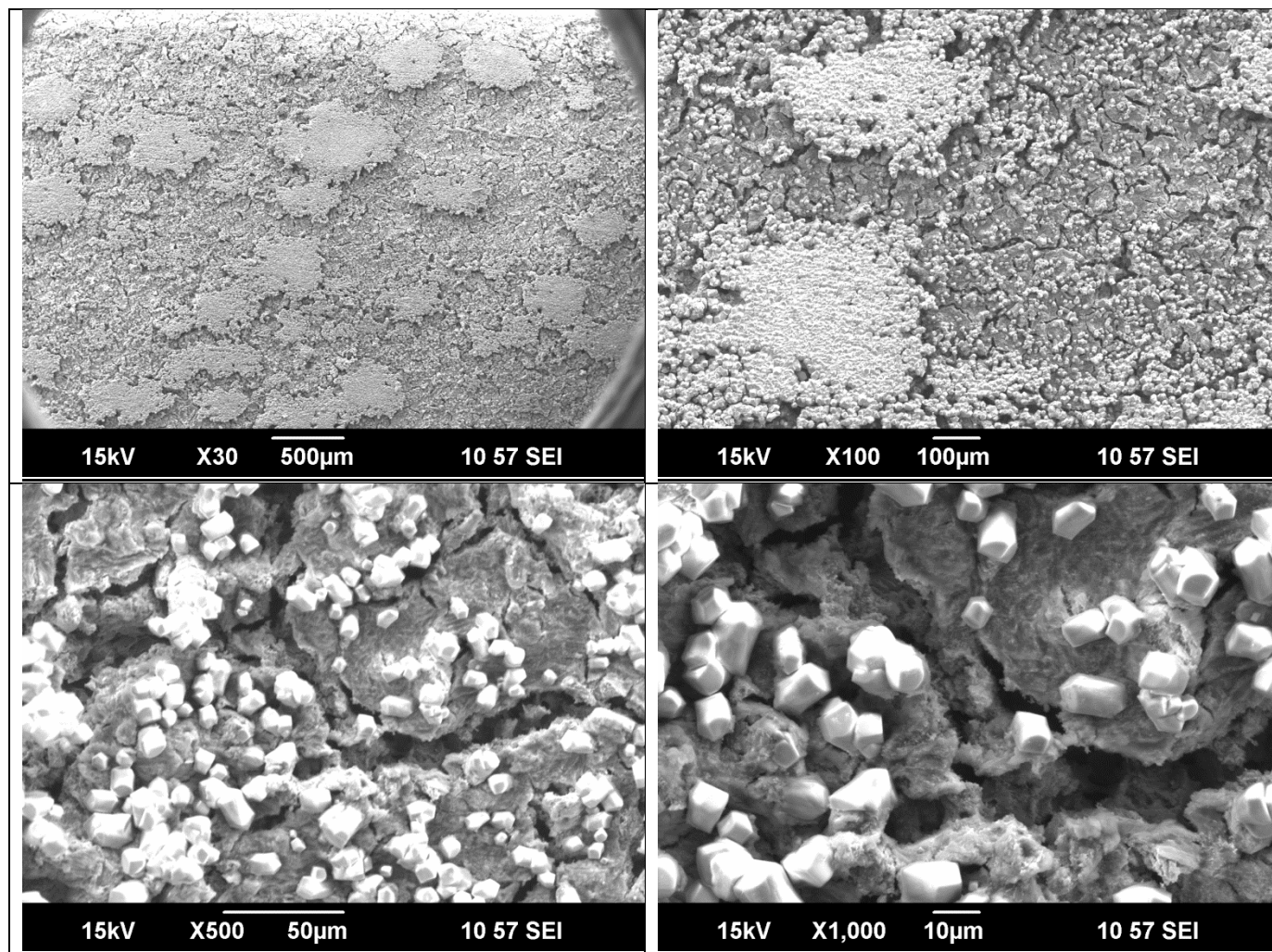


**Figure 4:** SEM images of steel specimen surface after experiments at Condition 3.  
 $T=80^\circ\text{C}$ ,  $p\text{CO}_2=10$  bar, and autogeneous pH.

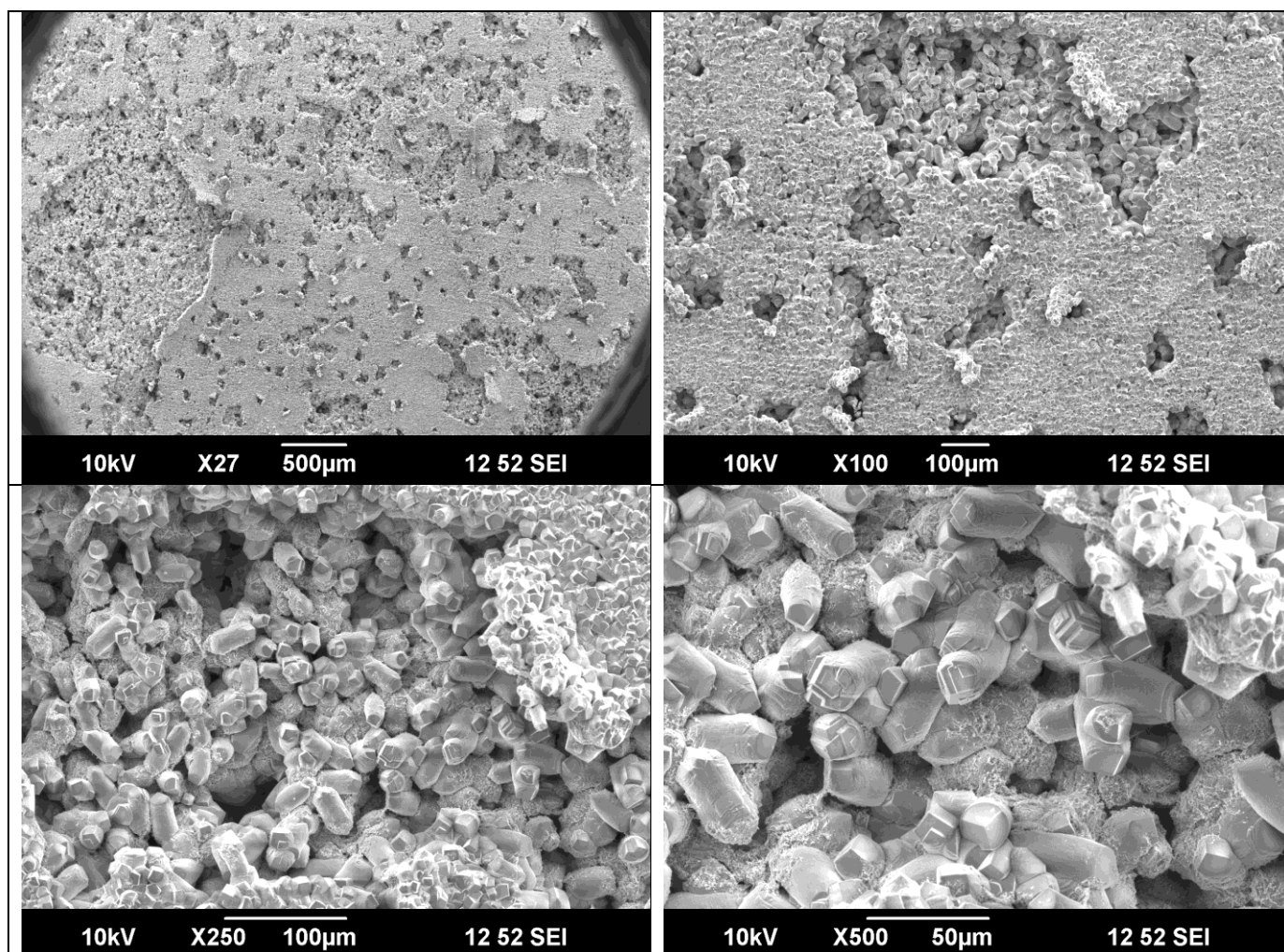


**Figure 5:** SEM images of X65 steel specimen surface after experiments at Condition 4.  
 $T=80^{\circ}\text{C}$ ,  $p\text{CO}_2=80$  bar, and autogeneous pH.

The elemental analysis of the steel surface with the corrosion product layer in place as well as cross section of the specimen revealed the  $\text{FeCO}_3$  present and adhering tightly to the steel surface. Figure 6 show the elemental analysis obtained by using the EDAX technique, with the peaks suggesting the formation of  $\text{FeCO}_3$ . The XRD analysis shown in Figure 7 confirmed the compound to be  $\text{FeCO}_3$ .



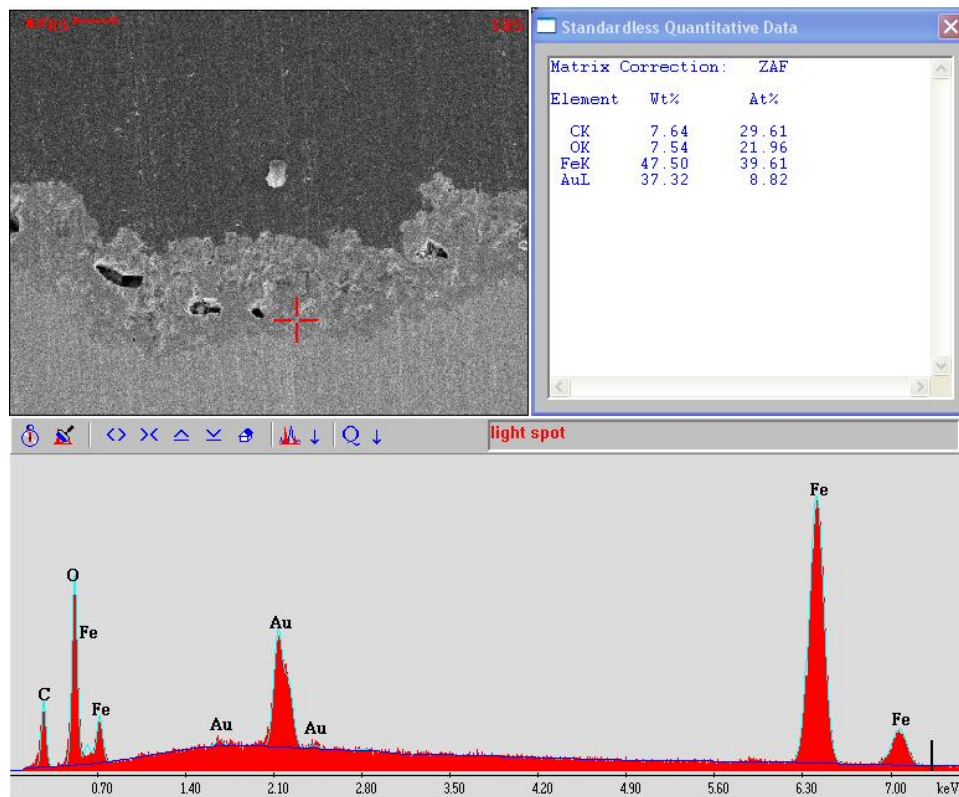
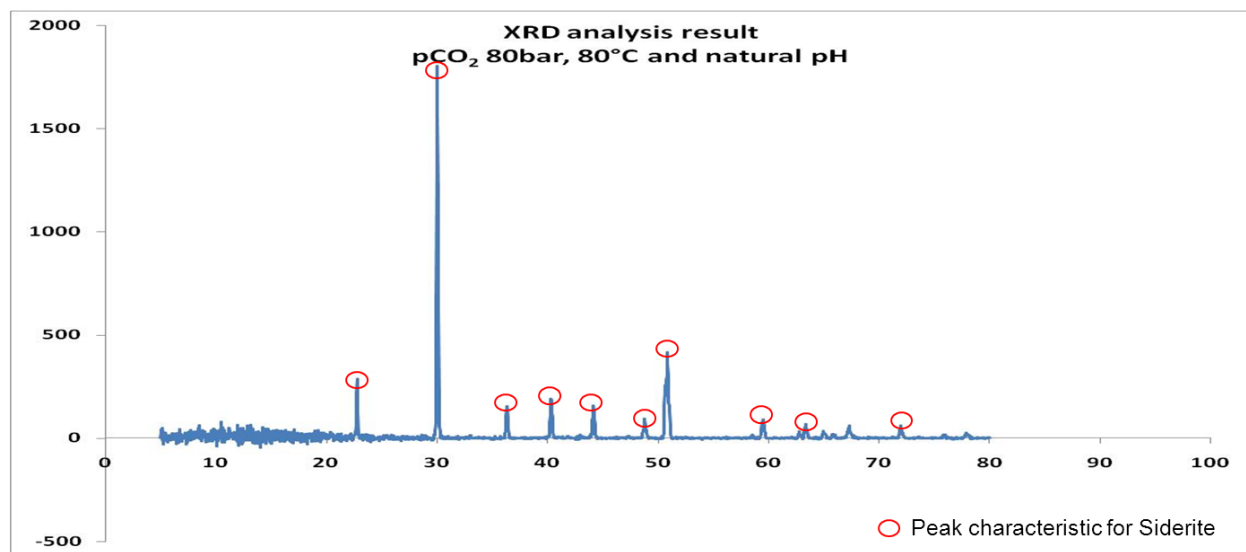


**Figure 6:** Elemental analysis obtained using EDAX analysis of X65 mild steel specimen's cross section after corrosion test at Condition 4.  $T=80^{\circ}\text{C}$ ,  $p\text{CO}_2=80$  bar and autogeneous pH.



Reference from Siderite XRD data, American Mineralogist 46 (1961) 1283-1316

**Figure 7:** X-Ray Diffraction Spectroscopy(XRD) analysis of X65 mild steel specimen's surface after corrosion test at Condition 4.  $T=80^{\circ}\text{C}$ ,  $p\text{CO}_2=80$  bar and autogeneous pH.

The above tests were done with a 24 hours of exposure. Further investigation was done at longer duration, up to 2 weeks to see if the protective effect of  $\text{FeCO}_3$  layer on corrosion of mild steel in high  $p\text{CO}_2$  will persist. Given the high volume of the autoclave, the water chemistry of the system did not change significantly in the longer duration experiment, as indicated by the pH increase from 3.2 to 3.8. Figure 8 shows that the corrosion rate was reduced to below 0.1mm/year within the first 2 days and

stayed low until test was completed. The corrosion rate from weight loss measurement yielded a time averaged corrosion rate of 2.7 mm/yr which agreed well with the LPR results.

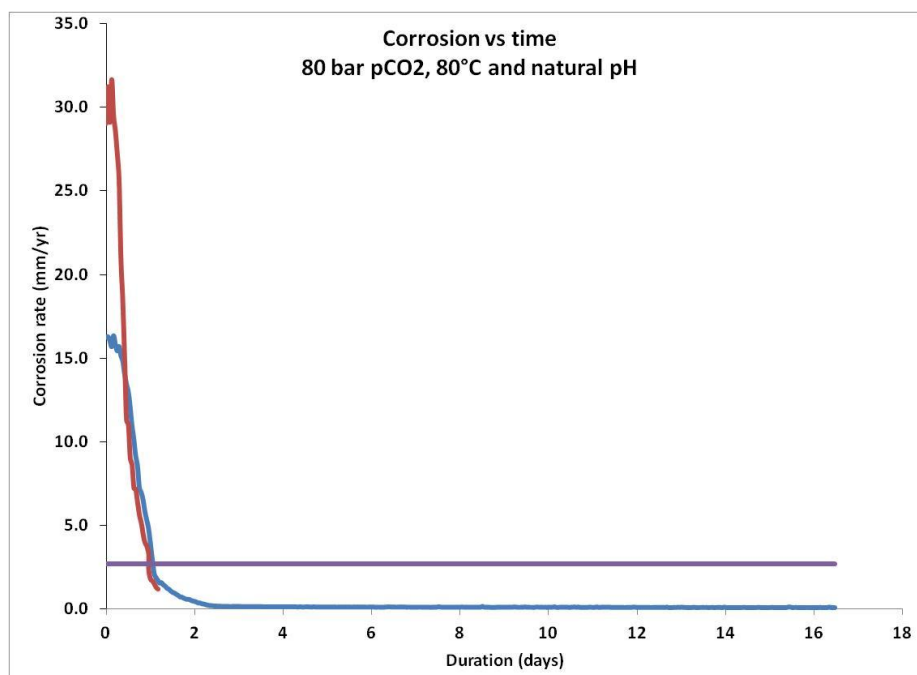


**Figure 8:** Long term LPR corrosion rate vs. time at Condition 4. T=80°C, pCO<sub>2</sub>=80 bar and autogeneous pH.

Overall the results highlight the effect of FeCO<sub>3</sub> layer on mild steel in high pCO<sub>2</sub> environments as summarized in Figure 9. The protectiveness of the layer was seen at pCO<sub>2</sub> above 70 bar, in the presence of the supercritical CO<sub>2</sub> phase. The other conditions did not show any reduction in corrosion rate over time although FeCO<sub>3</sub> was found on the steel surface. These results should be used with caution, as the effect of flow was not included in this study.



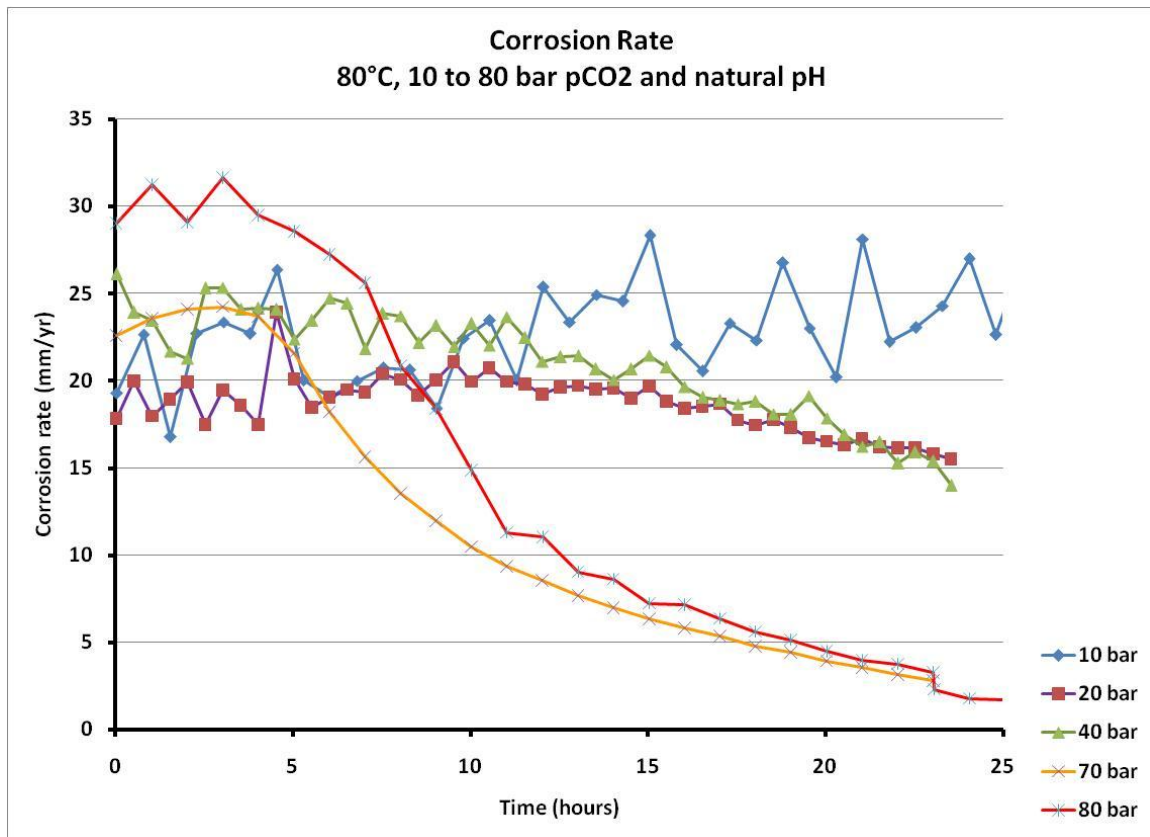


**Figure 9:** Corrosion rates plot vs. time for corrosion experiments at high temperature (80°C),  $p\text{CO}_2$  range from 10 bar to 80 bar and pH at autogeneous (3.2 to 3.8).

## CONCLUSIONS

This paper highlights the influence of  $\text{FeCO}_3$  layer formation during X65 mild steel corrosion in a high  $p\text{CO}_2$  environment. It was found that:

- Similar as in low  $p\text{CO}_2$  environments, the  $\text{FeCO}_3$  precipitation is very much temperature dependant.<sup>[9]</sup>
- Protective  $\text{FeCO}_3$  layer can deposited on mild steel surface in high  $p\text{CO}_2$  environment, even though the bulk pH is low, due to a much higher pH at the surface.
- The  $\text{FeCO}_3$  layer formed in supercritical  $\text{CO}_2$  conditions is able to suppress the corrosion rate to very low levels, i.e. below 0.1mm/yr.
- The formation of  $\text{FeCO}_3$  did not promote localized corrosion in high  $p\text{CO}_2$  environments.

## ACKNOWLEDGEMENTS

The authors would like to extend their deep appreciation and gratitude to PETRONAS for its financial support, Dr Sa'adan Mat for initiating and supporting the project, Al Schubert for designing the experimental setup, Mr. Cody Shafer helping fabricate and assemble the equipment, and the rest of the ICMT technical support team.

## REFERENCES

- [1] J. Veron, "An overview of the non-developed gas reserves in Southeast Asia," *PetroMin*, pp. 22-28, 2007.
- [2] C. de Waard and D. E. Milliams, "Carbonic acid corrosion of steel," *Corrosion*, vol. 31, pp. 177-188, 1975.
- [3] E. W. J. van Hunnik, B. F. M. Pots and E. L. J. A. Hendriksen, "The formation of protective  $\text{FeCO}_3$  corrosion product layers in  $\text{CO}_2$  corrosion," in *Corrosion/96*, Paper 6, (Houston, TX: NACE International), 1996.
- [4] Y. Choi and S. Nesic, "Corrosion behavior of carbon steel in super critical  $\text{CO}_2$ -water environments," in *Corrosion/09*, Paper 256, (Houston, TX: NACE International), 2009.
- [5] S. Nesic, "Key issues related to modeling of internal corrosion of oil and gas pipelines – A review," *Corrosion Science*, vol. 49, pp. 4308-4338, 2007.
- [6] W. Sun. (2006, November). Kinetics of iron carbonate and iron sulfide scale formation in  $\text{CO}_2/\text{H}_2\text{S}$  corrosion. *PhD Dissertation, Ohio University*.
- [7] S. Nesic, M. Nordsveen, R. Nyborg and A. Stangeland, "A mechanistic model for  $\text{CO}_2$  corrosion with protective iron carbonate films," in *Corrosion*, 2001.
- [8] A. Dugstad, "Mechanism of protective film formation during  $\text{CO}_2$  corrosion of carbon steel," *CORROSION 98*, 1998.
- [9] S. Nesic and J. Postlethwaite, "Modelling of  $\text{CO}_2$  corrosion mechanisms," *Corrosion*, vol. 266, pp. 317-335, 1994.